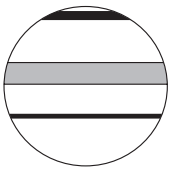

Research paper

Late Weichselian and Holocene sedimentary palaeoenvironment and glacial activity in the high-arctic van Keulenfjorden, Spitsbergen

The Holocene
0(0) 1–12

DOI: 10.1177/0959683613499055
hol.sagepub.com

Philipp Kempf,[1,2] Matthias Forwick,[1] Jan Sverre Laberg[1] and Tore O Vorren[1,*]

Abstract

High-arctic fjords, for example, van Keulenfjorden on Spitsbergen, provide valuable palaeoenvironmental archives as they typically contain landforms and sediment sequences that document past changes in glacial activity with high temporal resolution. Van Keulenfjorden was covered with a grounded glacier during the last glacial, and it was deglaciated between *c.* 11.8 and 11.3 cal. ka BP. The retreat of the ice front accelerated from approximately 80 to 190 m/a during the deglaciation. The maximum late Holocene glacier extent occurred after surge-like advances of the glacier Nathorstbreen between 2790 and 2610 cal. yr BP (i.e. during a period with the coldest climatic conditions on Svalbard). This maximum extent was reached approximately 2600 years earlier than inferred for most fjords on Svalbard, suggesting that surge-like glacier advances on Svalbard can occur under variable climatic conditions. The time interval between the advances of Nathorstbreen around 2.7 ka BP was approximately 100–150 years. This is comparable to the last and only historically known quiescent phase of Nathorstbreen of *c.* 120 years between the late 19th century and the most recent surge from 2003 to 2012.

Keywords

Arctic, deglaciation, fjord, glacial surge, late Weichselian–Holocene, sedimentary environment, Svalbard

Received 26 February 2013; revised manuscript accepted 2 July 2013

Introduction

High-arctic fjords (e.g. on Spitsbergen) provide valuable archives for the reconstruction of glacial activity with high temporal resolution, as they typically contain glacial landforms and postglacial sediment sequences (Forwick and Vorren, 2010). This includes deglaciation dynamics and glacial fluctuations in an interglacial setting.

West Spitsbergen fjords link the partially glaciated terrestrial environment with the open marine environment. Thus, they provide unique settings to study the interaction between the terrestrial and the marine realms. Although it is known that Svalbard is one of the clusters of surge-type glaciers on Earth (Hagen et al., 1993), knowledge of the glacial surge history on Svalbard is very limited. Surges occurred between the end of the Little Ice Age (LIA; *c.* AD 1900) and the present (e.g. Liestøl, 1977; Ottesen and Dowdeswell, 2006; Plassen et al., 2004). Only one known surge precedes the surges from the end of LIA (e.g. Hald et al., 2001; Kristensen et al., 2009). In this paper, we present seismic and sedimentological data to reconstruct fluctuations of the tidewater glacier Nathorstbreen in van Keulenfjorden, Svalbard, since the end of the last glacial, and we discuss how these fluctuations were related to past climate change and surge-like advances. In this paper, the term 'surge-like' is used to reflect surge advances and other surge-unrelated rapid glacial advances.

Physiographic setting

Van Keulenfjorden is located on southwestern Spitsbergen, Svalbard (Figure 1). It is 40 km long and up to 7.3 km wide. A prominent bedrock sill at the fjord mouth is at maximum 30 m deep and partially subaerial (Eholmen Island). A moraine complex in the middle of the fjord (Ottesen et al., 2008) subdivides van Keulenfjorden into an inner and an outer basin (Figure 1C).

The bedrock geology of the catchment area is dominated by the Central Spitsbergen Tertiary Basin containing rocks from the van Mijenfjorden group consisting mainly of shale, silt and sandstone of Palaeocene to Oligocene age. Folded and faulted, late Palaeozoic and Mesozoic sedimentary rocks of the West Spitsbergen fold and thrust belt surround the western parts of the fjord (Dallmann et al., 1990, 1994).

Sediment supply to Spitsbergen fjords occurs mainly from tidewater glaciers and glacial rivers (Elverhøi et al., 1983), and to a minor degree from sea-ice-rafting (Dowdeswell et al., 1998). Both subaqueous melt outwash and river discharge vary strongly with the melt season in spring (Svendsen et al., 2002). Sea ice can cover large parts of the fjord from late November until the middle of July (cf. Høyland, 2009).

The glacier coverage in the catchment area varies between 80% in the east and 50% in the west (Dallmann et al., 1994; Hagen et al., 1993). The largest glaciers surge episodically (Hagen et al., 1993; Hart and Watts, 1997; Jiskoot et al., 2000; Sund et al., 2009). Doktorbreen, Liestølbreen and Nathorstbreen (all surge-type; Figure 1C) are presently tidewater glaciers (Hagen et al., 1993).

*Deceased on 16 June 2013. This contribution is dedicated to Tore O Vorren.

[1]University of Tromsø, Norway
[2]Ghent University, Belgium

Corresponding author:
Philipp Kempf, Renard Centre of Marine Geology (RCMG), Ghent University, Krijgslaan 281, S8, 9000 Ghent, Belgium.
Email: philipp.kempf@ugent.be

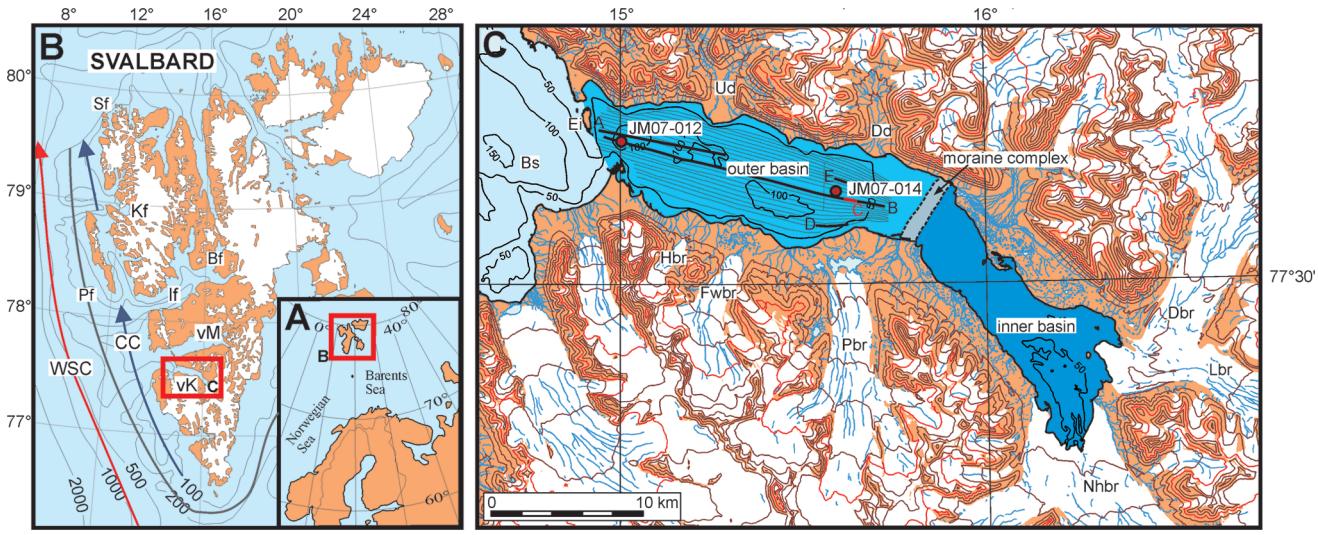

Figure 1. A: Overview map of the North Atlantic region, B: map of Svalbard with arrows indicating ocean currents and C: map of van Keulenfjorden with its outer and inner basins subdivided by a subaqueous moraine complex (grey area). Core locations are indicated by red dots. Thin grey lines are Chirp profiles, thicker lines with letters correspond to Chirp profiles displayed in Figure 3a–e.
Bs: Bellsund; Bf: Billefjorden; CC: coastal current; Dbr: Doktorbreen; Dd: Davisdalen; Ei: Eholmen island; Fwbr: Finsterwalderbreen; Hbr: Hessbreen; If: Isfjorden; Kf: Kongsfjorden; Lbr: Liestølbreen; Nhbr: Nathorstbreen; Pf: Polarfront; Ud: Ulladalen; vK: van Keulenfjorden; vM: van Mijenfjorden; Pbr: Penckbreen; Sf: Smeerenburgfjorden; WSC: West Spitsbergen Current.

Late Weichselian and Holocene glacial history

West Spitsbergen fjords acted as pathways for fast-flowing ice streams draining the Late Weichselian Svalbard Barents Sea Ice Sheet (e.g. Landvik et al., 1998; Ottesen et al., 2005). In Bellsund (Figure 1), the ice stream draining through van Keulenfjorden merged with the ice stream draining through van Mijenfjorden and extended to the shelf break west of Spitsbergen during their maximum extents. The retreat of the ice fronts from their maximum extents began around 20.5 cal. ka BP (Jessen et al., 2010), and shortly after 14.5 cal. ka BP, the ice front retreated from Bellsund trough to the fjord mouths of van Keulenfjorden and van Mijenfjorden (Mangerud et al., 1992; Svendsen et al., 1996). The chronology of the deglaciation of van Keulenfjorden is poorly known, but it has been inferred that the neighbouring van Mijenfjorden was deglaciated between *c.* 12.1 (Mangerud et al., 1992) and 11.3 cal. ka BP (Hald et al., 2004).

Following the deglaciation of the fjords, a relatively warm period in the early Holocene with enhanced inflow of Atlantic Water (AW), reduced ice-rafting, as well as smaller tidewater and terrestrial glaciers prevailed on Spitsbergen (Baeten et al., 2010; Birks, 1991; Forwick et al., 2010; Forwick and Vorren, 2007, 2009; Hald et al., 2004; Rasmussen et al., 2012; Svendsen and Mangerud, 1997). Due to general climatic cooling, existing glaciers started to grow, and new glaciers formed asynchronously after *c.* 9.0 cal. ka BP (Forwick et al., 2010; Forwick and Vorren, 2007, 2009; Hald et al., 2004; Svendsen and Mangerud, 1997). This climatic cooling culminated between 4.7 and 2.0 cal. ka BP (Birks, 1991; Hald et al., 2004; Rasmussen et al., 2012; Skirbekk et al., 2010; Svendsen and Mangerud, 1997). However, other studies suggest few and small glaciers on land at the end of this period (Humlum et al., 2005). Most known maximum late Holocene glacier extents on Svalbard occurred during a final phase of the LIA due to increased mass balance (D'Andrea et al., 2012; Elverhøi et al., 1995; Mangerud and Landvik, 2007; Ottesen and Dowdeswell, 2006; Plassen et al., 2004). However, evidence of earlier advances has been found sporadically (Hald et al., 2001; Werner, 1993). Since approximately 1900 AD, the glacier fronts retreated, occasionally interrupted by surge advances (e.g. Plassen et al., 2004; Sund et al., 2009).

Material and methods

Swath-bathymetry, sub-bottom and high-resolution seismic profiles, as well as sediment cores from the outer basin of van Keulenfjorden provide the basis for this study. The data were collected in 1997, 2007 and 2009 with R/V *Jan Mayen*.

The swath-bathymetry data were acquired in October and November 2009 with a hull-mounted *Kongsberg Maritime Simrad EM 300 multibeam echo sounder* operating with a nominal frequency of 30 kHz. Processing and visualization was done using the softwares *Neptune* and *IVS 3D Fledermaus v. 7*. The data set is displayed with a grid cell size of 12 m.

Sub-bottom profiles were acquired simultaneously with the swath-bathymetry data, using a hull-mounted *EdgeTech 3300-HM Chirp sub-bottom profiler* with a band pass-filter setting of 2–12 kHz and a pulse length of 20 ms. Isopach maps were created from these data using the *SMT Kingdom Software v. 8.6*. Whenever a metric description of a sedimentary body or a geomorphologic feature is given, it refers to a p-wave velocity of 1500 m/s. Sparker data were collected in 1997 with a *700 J Bennex multi-electrode Sparker* and displayed with a pass filter of 150–700 Hz. A vertical resolution of 55 cm is achieved.

Sediment samples were retrieved from the sites JM07-012 and JM07-014 (Figure 1C) using a 6-m-long gravity corer and a 12-m-long piston corer, respectively. For both corers, steel barrels with an inner diameter of ~11 cm were attached to lead weights of approximately 1.6 tonne. The barrels were loaded with plastic liners with inner diameters of 10.2 cm. The liners were cut into approximately 1-m-long sections after recovery and then stored at +4°C.

Prior to opening of the cores, the gamma ray attenuation density, p-wave velocity and magnetic susceptibility were measured at 1 cm increments using a *GEOTEK Multi Sensor Core Logger* (MSCL). After the cores were split, X-radiographs of half-core sections were taken and described. Subsequently, visual description was performed. Grain-size distribution analyses are based on 1-cm-thick slices from half cores subsampled at approximately 10 cm intervals. For the grain-size analysis, sieves with mesh sizes of 2 mm, 1 mm, 500 µm, 250 µm, 125 µm and 63 µm were used. The <63 µm fraction was analysed with a *Micromeritics SediGraph 5100* after treating the sample with sodium hexametaphosphate

Table 1. Sediment cores (see Figure 1 for location).

Core ID	Latitude (°N)	Longitude (°E)	Water depth (m)	Core length (m)
JM07-012-GC	77°35.12′	014°59.95′	100	2.70
JM07-012-PC	77°35.07′	015°00.73′	101	3.82
JM07-014-PC	77°33.33′	015°35.29′	82	5.38

GC: gravity core; PC: piston core.

and ultrasound. The shear strength was measured approximately every 5 cm using the fall-cone test after Hansbo (1957). A composite core log was compiled from a gravity and a piston core at site JM07-012 (Table 1).

The chronologies for the cores are based on 14 samples of bivalve, gastropod and brachiopod shells and bryozoans that were radiocarbon dated at the *Poznan Radiocarbon Laboratory*, Poland, and at *The ^{14}Chrono Centre for Climate the Environment and Chronology* in Belfast, UK. The results were calibrated with the software Calib 6.0 (Stuiver et al., 2010) using $\Delta R = 105 \pm 24$ years to account for reservoir age effects (Mangerud et al., 2006). The results were obtained from the marine09.14c calibration curve (Reimer et al., 2009). They are reported in calibrated years before present (cal. yr BP). Radiocarbon dates from literature were re-calibrated using the same parameters of this study for better comparability (Table 2).

Results

A regional seismostratigraphy is established by strongly building on already existing seismostratigraphies from other Spitsbergen fjords. The geomorphological features are described in detail within their stratigraphic context. The lithological results and age control are presented once the geo-acoustic results have introduced the sedimentary architecture of the fjord.

Regional seismostratigraphy and subaqueous landforms

Six seismostratigraphic units are defined in outer van Keulenfjorden on the basis of acoustic characteristics (e.g. internal signature and geometry; cf. Syvitski and Praeg (1989)). The stratigraphy was established at acoustically characteristic sections and subsequently traced laterally to describe the regional seismostratigraphy. It should be noted that local variations in acoustic characteristics, internal signature and unit geometry occur (cf. Carlson, 1989; Forwick and Vorren, 2010; Syvitski and Praeg, 1989; Vorren et al., 1989). Whereas the lowermost unit VK0 is described from sparker data (Figure 3a), the description of all remaining units is based on acoustic characteristics on Chirp sub-bottom profiles (Figure 3b–e). The seismostratigraphic units from van Keulenfjorden correlate with the seismostratigraphy for the Isfjorden system, the largest fjord system on Svalbard (Forwick and Vorren, 2010). An overview of the characteristics of the seismostratigraphic units is presented in Table 2.

Bedrock-controlled ridges and basins. Up to 1.7-km-wide north-northwest–south-southwest (NNW-SSE) oriented ridges and up to 4.0-km-long basins control the large-scale bathymetry of the outer fjord basin (Figure 2). The water depths of the ridges and the basins range between approximately 105 and 65 m. The orientation of these features, as well as the absence of evidence that the ridges are depositional features suggest that they are sea floor expressions of the underlying bedrock belonging to the West Spitsbergen fold and thrust belt (Dallmann et al., 1990).

Seismo-unit VK0. Unit VK0 is the lowermost recognized unit that generally drapes the bedrock/acoustic basement, is a few-meters thick and has a semi-transparent to chaotic internal signature (Table 2). However, close to the fjord mouth, it thickens to an approximately 50-m-thick, acoustically semi-transparent wedge-shaped deposit that laps onto the fjord-mouth bedrock sill. The limited penetration by the Chirp signal is probably due to a diamictic composition of the sediment (Stewart and Stoker, 1990).

Because grounded glaciers typically erode into and remove preglacial deposits (Hooke and Elverhøi, 1996) and due to the location of unit VK0, on top of acoustic basement, we suggest that the deposits are of subglacial origin and that they were deposited during the last glaciation (Figure 2). However, the occurrence of internal reflections (Figure 3a) may indicate that deposits predating the last glacial are also preserved (cf. Forwick and Vorren, 2010; Mangerud et al., 1998). While the thinner part in the east has many characteristics of a subglacial till (opaqueness, chaotic to discontinuous reflections), the available data do not allow an unequivocal determination of the formation mechanisms of the thicker part of this unit.

Seismo-unit VK1. Seismo-Unit VK1 was deposited in the entire outer basin and overlies unit VK0 (cf. Bratlie, 1994). A 7.5-km-long, 150-m-wide (and on average 2 m high) single ridge, oriented subparallel to the fjord axis, is located in the eastern part of the outer basin (Figure 2). In the east, the ridge is straight and connects 12 beads reaching 14 m in height. The beads are symmetrical in both cross and long profile. The original, unburied height of the ridge and beads is between 1.5 and 2 times their height on the current sea floor. To the west, the ridge becomes zigzagged to sinuous. Due to its morphology and stratigraphic position, this landform is inferred to be a beaded esker (cf. Warren and Ashley, 1994) that was deposited during the deglaciation. The beads line up because of the relatively fixed position of a subglacial meltwater conduit supplying the sediment. This conduit probably originated from one of the confluences of Nathorstbreen, for example, Liestølbreen or Doktorbreen (cf. Liestøl, 1977). The beads are either subaqueous ice-contact outwash fans or small moraines created during halts or minor re-advances during the deglaciation (Diemer, 1988; Henderson, 1988).

VK1 also contains 2–4 m high ridges with crest spacing of 80–190 m (Figure 3e). These ridges correspond to two groups of comparatively small ridges on the present fjord floor (Figure 2): (1) up to 1.5-m-high, subparallel, and relatively linear, transverse ridges visible with an average spacing of 80 m in the middle of the fjord (south and southeast of Ulladalen); (2) v-shaped ridges of 2 m height with an average spacing of 190 m in the eastern parts of the basin (Figure 2). The apexes of the v-shaped ridges always coincide with a mound of the beaded esker. Both groups of ridges have a quasi-regular distribution in their areas of occurrence. The inclusion into seismo-unit VK1 and the relation to the esker beads indicate a glacigenic origin from the last glacial. They are interpreted to be moraines that were formed during repeated halts or minor re-advances of the ice front during overall deglaciation.

A sinuous ridge merges with the beaded esker in the eastern part of the study area (Figure 2). It is 2-km-long, on average 80-m

Table 2. Characteristics of the seismostratigraphic units.

Name	Maximum thickness	Average thickness	Unit geometry	Lower boundary	Upper boundary	Acoustic signature	Age constraints	Interpretation	Corresponding Isfjorden unit[a]	Isfjorden unit interpretation[a]
VK5	37 m	7 m	Westward thinning	Transitional, continuous	Sharp, continuous (sea floor)	Stratified, continuous	At least since 2930 yr BP to present	Glacimarine mud	Upper S6	Mid- to late Holocene glacimarine deposits
VK4	12 m	5 m	Westward thinning	Transitional, continuous	Transitional, continuous	Stratified, continuous	–	Glacimarine mud	Lower S6	Mid- to late Holocene glacimarine deposits
VK3	17 m	9 m	Thinner on ridges, thicker in depressions/basins	Sharp, discontinuous	Transitional, continuous	Transparent to weakly stratified, discontinuous	–	Glacimarine mud	S5	Early Holocene glacimarine deposits
VK2	6 m	2 m	Trough infill between ridges of VK1, sometimes missing on crests	Sharp, discontinuous	Sharp, discontinuous	Thickly stratified, discontinuous	During and shortly after deglaciation, 11.8–11.3 ka BP	Proglacial outwash	S4a	Late Weichselian or earliest Holocene stratified glacimarine deposits
VK1	3 m	2 m	Sometimes forms ridges, drape on VK0	Sharp, continuous	Sharp, discontinuous	Semi-transparent, chaotic	Deglaciaion, c. 11.8–11.3 ka BP	Proglacial diamicton	S2	Late Weichselian or earliest Holocene glacier-frontal deposits
VK0	50 m	20 m (2 m in the east)	Lobe shaped in the west and thin in the east	Sharp, discontinuous	Sharp, continuous	Semi-transparent, chaotic	Last glacial or older	Subglacial diamicton	S1	Late Weichselian or earliest Holocene subglacial deposits

[a]Isfjorden stratigraphy correlation based on Forwick and Vorren (2010).

Figure 2. (a) Swath-bathymetry map surrounded with the geological map from Dallmann et al. (1990), in which yellow colours represent the Central Spitsbergen Tertiary Basin and colours ranging from blue and purple to green represent the groups, which are comprised in the West Spitsbergen Fold and Thrust Belt. Dashed black lines indicate bedrock ridges belonging to the fold and thrust belt and (b) landform interpretations based on the swath bathymetry presented in (a).

wide and emerges 2 m from the present sea floor. However, on the surface of seismo-unit VK1, it has a height of approximately 6 m. Its height, width and the shape of the cross-profile are constant along the ridge. Close to its southeastern, up-fjord end, the ridge turns approximately 160° from SW to N across ice flow direction and is mostly oriented transverse to the fjord axis. Because this ridge is limited by the beaded esker, and because it belongs to seismo-unit VK1, we suggest that it is an esker, too. The transverse orientation is unusual, but transverse eskers have been described before (e.g. Evans and Twigg, 2002).

Seismo-unit VK2. Unit VK2 is up to 6 m thick and acoustically stratified. It fills the depressions between the ridges of VK1 and is typically thinner, sometimes absent, on top of the crests (Figure 4c). This results in a general smoothening of the relief of VK1. The acoustic stratification is suggested to reflect frequent lithological changes in a glacier-proximal environment (cf. Forwick and Vorren, 2010; Gilbert and Barrie, 1985; Syvitski and Praeg, 1989).

Seismo-unit VK3. The acoustically transparent to weakly stratified unit VK3 is deposited in the entire outer basin, where it drapes unit VK2 as an unconformable layer (Figure 4c). Its large-scale geometry is mainly controlled by the distribution of bedrock basins and ridges resulting in thicker deposits in the basins (Figure 5a). In the westernmost parts of the study area, it becomes indistinguishable due to a generally chaotic acoustic signature.

The acoustically transparent to weakly stratified signature is interpreted to result from a relatively homogenous and muddy composition of the sediment reflecting a relatively stable glacimarine environment with reduced ice-rafting (e.g. Forwick and Vorren, 2009, 2010; Hald et al., 2004). However, the reflections

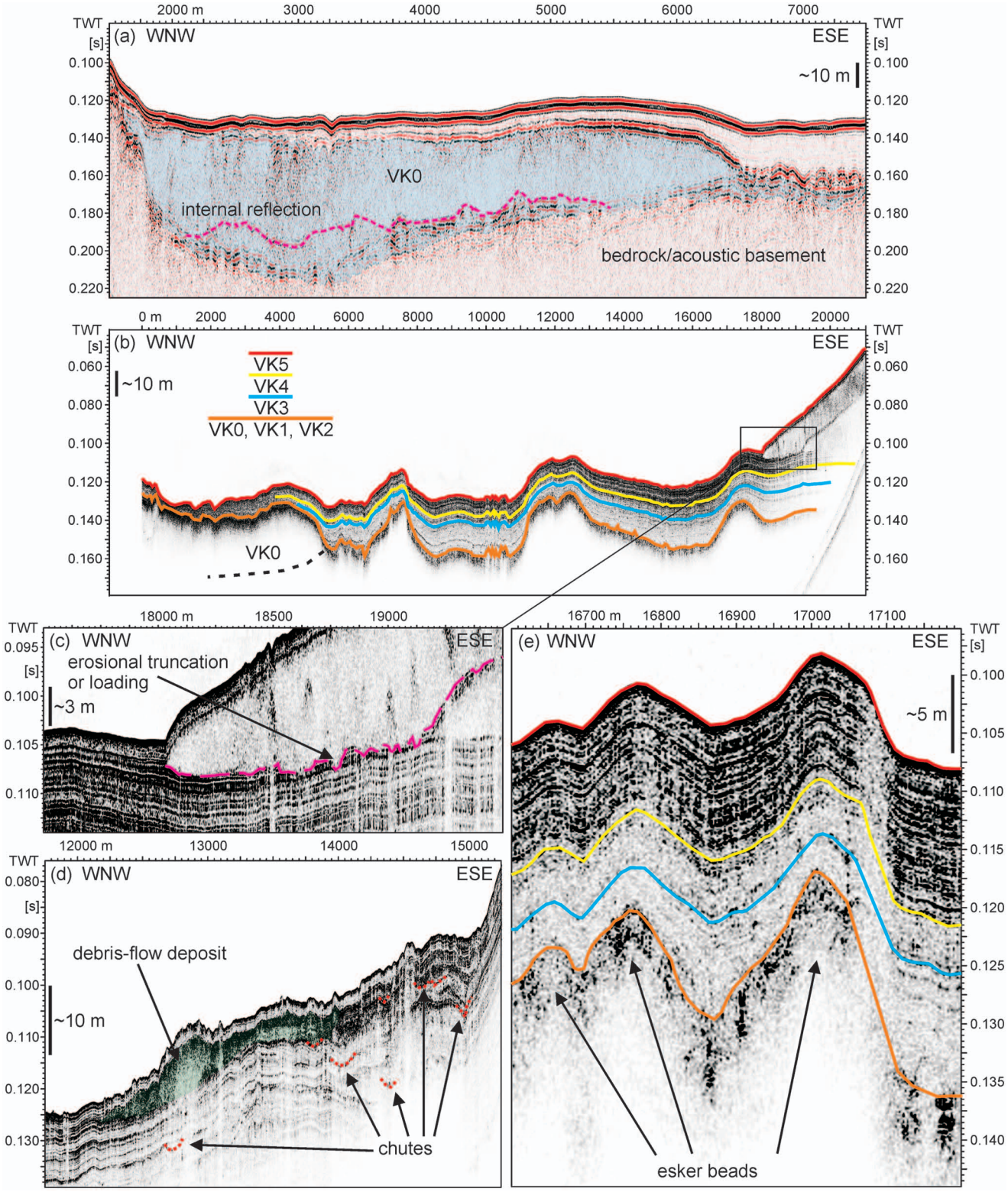

Figure 3. Selected high-resolution seismic profiles. The exact line positions are displayed in Figure 1. (a) Sparker profile from the western part of the outer basin and (b) representative Chirp profile along the fjord axis in the outer basin. The upper and lower boundaries of the seismostratigraphic units are indicated with solid coloured lines; (c) zoom-in showing the talus of debris-flow wedges. The pink dashed line indicates the erosional truncation or loading characteristic of the lower boundary of the upper debris lobe; (d) Chirp profile along the fjord axis off Penckbreen displaying evidence of downslope sediment transport and (e) Chirp profile through three beads showing that their origin is below the postglacial sedimentary succession.

are attributed to ice-rafted debris (IRD)-rich intervals deposited from occasionally enhanced ice-rafting.

Seismo-unit VK4. Continuous acoustic and stronger stratification than in unit VK3 characterizes the westward thinning unit VK4 that occurs in the entire outer basin (Figures 4c and 5b). Thicker and acoustically more diffuse and chaotic deposits occur repeatedly in the units VK4 and VK5 in front of sandur deltas and glaciers along the fjord sides (e.g. off Ulladalen and Finsterwalderbreen; Figure 3d). VK4 is inferred to have been deposited in a glacimarine environment. More frequent, stronger and continuous acoustic stratification than in VK3 reflects periods of enhanced

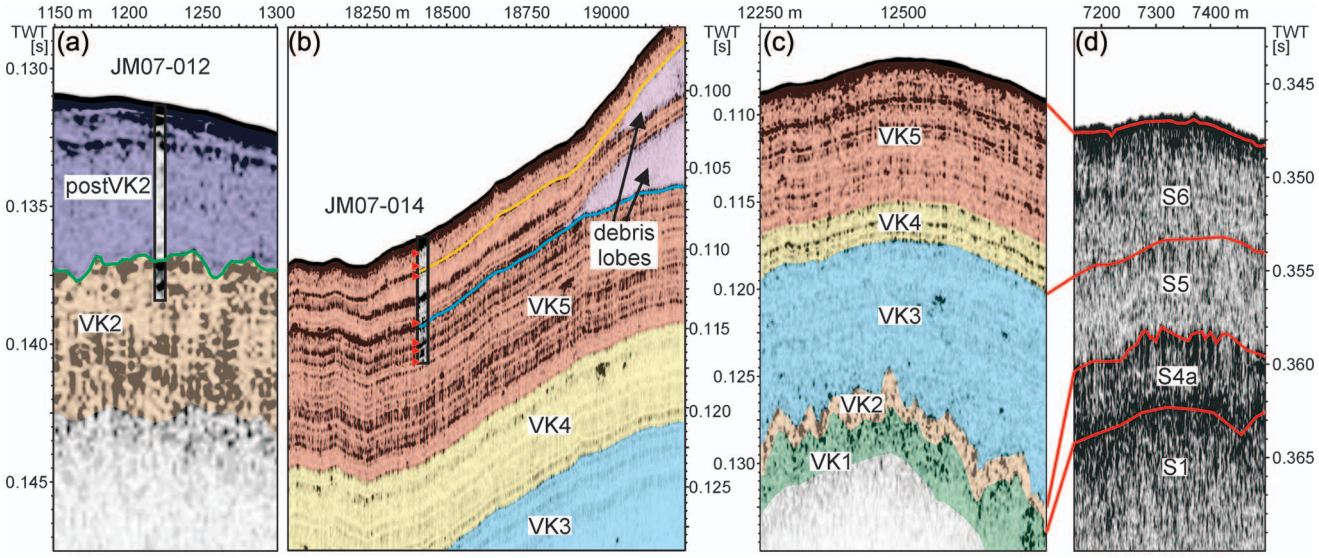

Figure 4. Zoom in on the Chirp profiles at core sites (a) JM07-012 and (b) JM07-014. The calculated core depth is indicated with a black outline. The green-, yellow- and blue-lined horizons in (a) and (b) are correlated to lines of identical colour in the lithology in Figure 6. Red triangles indicate radiocarbon dated macrofossils; (c) characteristic section of a Chirp profile to illustrate the defined seismostratigraphic units of the outer basin and (d) 3.5 kHz penetration echo sounder profile illustrating the established seismostratigraphic units from Isfjorden. The red lines on (d) correlate the seismostratigraphy from van Keulenfjorden with the seismostratigraphy from Isfjorden (from Forwick and Vorren, 2010).

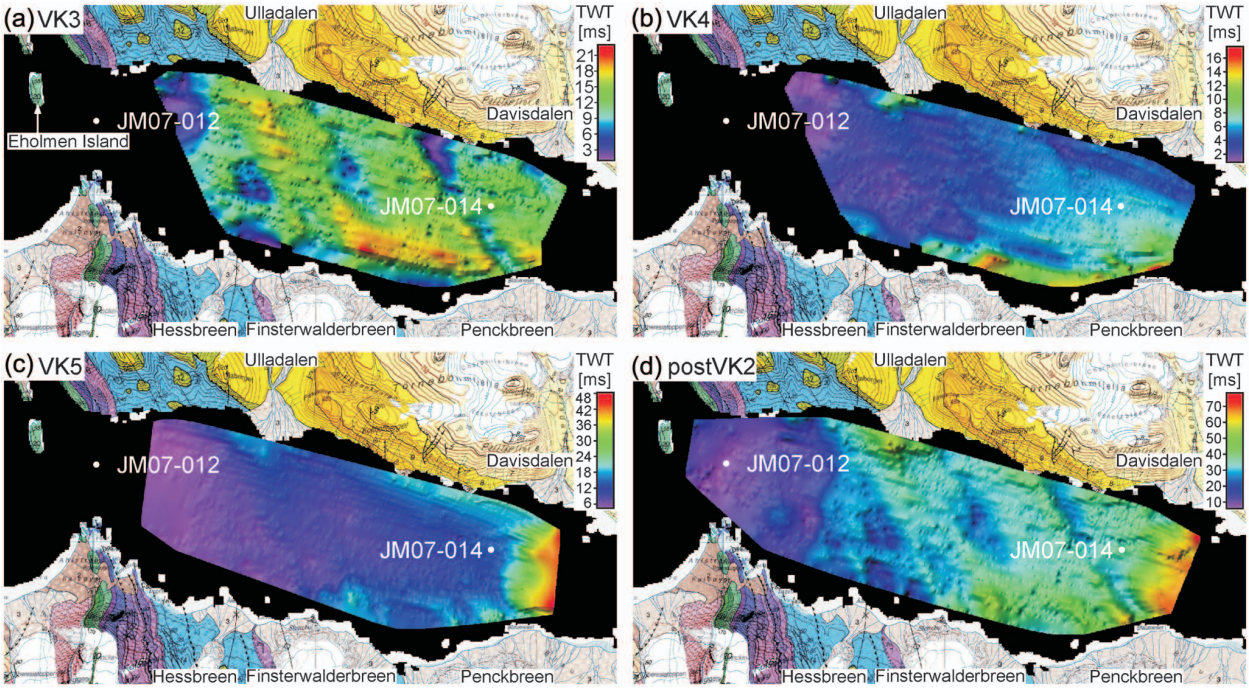

Figure 5. Isopach maps of (a) VK3, (b) VK4, (c) VK5 and (d) the entire post-VK2 succession. The surrounding geological map is from Dallmann et al. (1990).

ice-rafting (Forwick and Vorren, 2010). The more diffuse and chaotic deposits are interpreted as mass-transport deposits (Forwick and Vorren, 2012).

Seismo-unit VK5. The acoustically well stratified unit VK5 is the uppermost seismostratigraphic unit (Figure 4c). It occurs in the entire outer basin and thins westward. However, locally thicker accumulations occur in the vicinities of sediment sources along the fjord sides, for example, Penckbreen and Davisdalen (Figure 5c). The unit is interpreted to be deposited in a glacimarine environment. Strong reflections most probably reflect more intense ice-rafting than during the deposition of unit VK4.

Multiple acoustically transparent sediment bodies occur in this unit. The most dominant features are two sediment wedges in the easternmost part of the outer basin, on the distal side of the moraine complex that bisects van Keulenfjord into the inner and the outer basin (Figures 2, 3b–c and 4b). The upper and lower wedges are at least up to 23 and 15 m thick, respectively, and separated by a 1.5- to 2.25-m-thick interval of acoustically stratified deposits. These wedges have a semi-circular surface expression and are 4.5 km wide, 5 km long and gently westward-dipping (0.75°). Circular depressions with raised rims and diameters of up to 50 m are pockmarks resulting from dewatering due to rapid deposition of the sediment wedge (Forwick et al., 2009; Ottesen

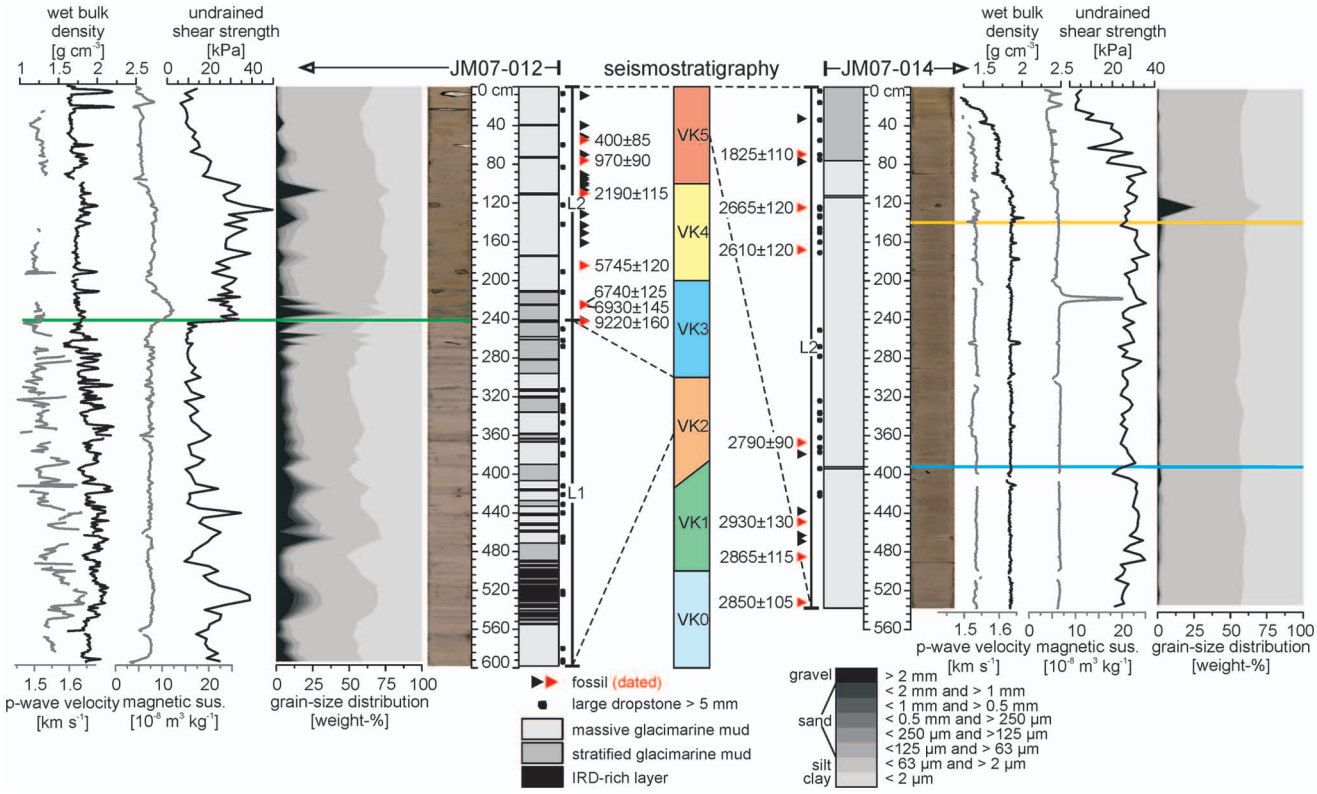

Figure 6. Physical properties, grain-size distributions, colour images, lithological logs and radiocarbon dates obtained from the cores JM07-012 and JM07-014, as well as the correlation of lithostratigraphy and seismostratigraphy. The green line on core JM07-012 and the yellow and blue lines on core JM07-014 correspond to the green-, yellow- and blue-lined horizons in Figure 4a and b.

et al., 2008). The acoustic signature beneath the pockmarks (Figure 2) is characterized by a cloud of chaotic high-magnitude reflections causing a strong acoustic masking effect below. The bases of the wedges either eroded into or compacted the underlying deposits. Ottesen et al. (2008) have interpreted these as debris-flow lobes and suggest tentatively that they resulted from slope failure on the distal side of a terminal moraine deposited by a surge advance of Nathorstbreen in the late 19th century. The age–depth model in combination with the correlation between the core and the sub-bottom profile shows that both lobes are older than the late 19th century (see below). It remains, however, unclear whether the debris-flow lobes were formed in association with a surge advance, or a rapid, non-surge advance.

Lithostratigraphy

Two core sites are located in the outer basin (Figure 1). Core JM07-012 is located in the westernmost part, where a thin post-glacial sediment cover allowed the penetration into deposits from the last glacial (Figures 4a and 5d). Core JM07-014 is situated just beyond the distal side of the debris lobes allowing the penetration of sediments deposited synchronously with the debris-flow deposits (Figure 4b).

Litho-unit L1. Unit L1 is the lowermost lithological unit that was exclusively recovered from core site JM07-012 (Figure 6). It is at least 3.55 m thick and composed of dark greyish brown to very dark grey (Munsell Soil Color Chart, MSCC 2.5Y 4/2 to 2.5Y 3.5/1) massive and stratified clayey silt. Relatively large amounts of lithic clasts occur either as single grains or in strata occur. The clasts are interpreted to be IRD. Macrofossils are absent, and benthic foraminifera are only found sporadically. The lower boundary of the unit was not recovered in our cores. However, the upper boundary is sharp, possibly erosional.

The lithological stratification and the IRD-rich layers point towards a highly dynamic (rapid sedimentation) glacimarine environment, which could be the cause for the lack of fossils. Colour changes may reflect changes in the sediment composition deriving from a single glacier front and/or sediment input from multiple sources (cf. Forwick and Vorren, 2009). Unit L1 is interpreted to have been deposited in a glacier-proximal environment.

Litho-unit L2. Unit L2 comprises the entire core JM07-014 and the upper 244 cm of core JM07-012 (Figure 6). Its upper boundary is the sea floor; its lower boundary (in core JM07-012) is sharp. Massive, dark olive grey to very dark greyish brown (MSCC 5Y 3/2 to 2.5Y 3/1) clayey silt with intervals of higher clast content and sporadic stratification characterize the unit. Macrofossils occur frequently, and benthic foraminifera are ubiquitous. At core site JM07-014, the laminations are generally weaker, and IRD content is lower than at site JM07-012.

The occurrence of clasts is suggested to reflect ice-rafting from icebergs and sea ice. However, the abundance of IRD-rich intervals and lithological changes are generally less frequent in unit L2 compared to unit L1. Furthermore, the increased abundance of tests from macro- and micro-organisms reflects more favourable living conditions during the deposition of unit L2. Unit L2 is interpreted to have been deposited in a more glacier-distal environment than unit L1 (cf. Forwick and Vorren, 2009).

Correlation of seismostratigraphy and lithostratigraphy. Based on the acoustic and lithological properties, we suggest the following correlation of seismostratigraphy and lithostratigraphy (Figures 4 and 6). At core site JM07-012, unit L1 is correlated with VK2, based on the acoustic and lithological stratifications, respectively. The boundary between L1 and L2 is correlated to the boundary between VK2 and the overlying deposits (VK3, VK4 and/or VK5

Table 3. Radiocarbon ages and calibrated ages obtained from the cores analysed in this study, as well as selected published ages.

Core ID or location	Depth (cm)	Material	Laboratory no.	^{14}C age (^{14}C years)	Calibrated age (2σ) (yr BP)	Origin
JM07-012-GC	55	*Chlamys islandica*	UBA-18483	890 ± 29	320–492	This study
JM07-012-GC	76	*Turritellidae*	Poz-37307	1520 ± 30	883–1058	This study
JM07-012-GC	111	Fragments of *Macoma calcarea* and *Astarte montagui*	UBA-18479	2621 ± 30	2075–2301	This study
JM07-012-GC	186	bryozoan – probably *Myriapora sp.*	UBA-18481	5471 ± 35	5622–5863	This study
JM07-012-GC	225	*Nuculana minuta*	Poz-37306	6540 ± 40	6780–7073	This study
JM07-012-GC	244	Bryozoan – probably *Myriapora sp.*	UBA-18480	8670 ± 41	9059–9375	This study
JM07-012-PC	8	*Hemithiris psittacea*	Poz-37309	6380 ± 40	6617–6862	This study
JM07-014-PC	70	*Ennucula tenuis*	UBA-18478	2336 ± 30	1717–1932	This study
JM07-014-PC	125	*Cylichna alba*	Poz-39210	3025 ± 35	2542–2785	This study
JM07-014-PC	168	*Cylichna alba*	Poz-37308	2970 ± 30	2490–2729	This study
JM07-014-PC	368	*Cylichna alba*	Poz-39211	3115 ± 35	2703–2879	This study
JM07-014-PC	451	*Thyasira gouldi*	UBA-18484	3246 ± 33	2799–3058	This study
JM07-014-PC	485	*Thyasira gouldi*	UBA-18482	3197 ± 34	2752–2979	This study
JM07-014-PC	532	*Cylichna alba*	Poz-37310	3180 ± 35	2742–2955	This study
90-21-GCI	157–162	*Neogloboquadrina pachyderma*	TUa-359	15255 ± 175	17471–18537	Svendsen et al. (1996)
90-25-PCI	379	*Mollusc* (unidentified fragment)	TUa-356	12845 ± 100	13968–14965	Elverhøi et al. (1995) and Svendsen et al. (1996)
Brommeldalen	–	*Yoldiella lenticula, Portlandia arctica, Nucula tenuis* and *Macoma calcarea*	T-5368	10940 ± 200	11566–12684	Mangerud et al. (1992)
MD99-2305	1595–1596	*Nepenthes tenuis*	TUa-4318	10384 ± 45	11255–11396	Hald et al. (2004)
52/pc1	380–384	*Portlandia arctica*	GX-18547-AMS	10703 ± 122	11332–12328	Bratlie (1994)
Ytterdalen	–	*Hiatella* and *Mya*	T-4865	11460 ± 110	12627–13095	Landvik et al. (1987)
Ytterdalen	–	*Hiatella* and *Mya*	T-5410	11040 ± 130	12003–12677	Landvik et al. (1987)
Ytterdalselva	–	Whalebone	T-5665	8390 ± 120	8505–9178	Landvik et al. (1987)

UBA: ^{14}Chrono Centre for Climate, the Environment and Chronology, Belfast, UK; Poz: Poznan Radiocarbon Laboratory, Poland; TUa: the Svedberg Laboratory, Uppsala, Sweden; T: Radiological Dating Laboratory, Trondheim, Norway; GX: unknown laboratory.

that cannot be distinguished at the core site; Figures 3b, 4c and 6). Unit L2 at site JM07-014 is correlated to VK5.

Chronology, age–depth models and accumulation rates

All radiocarbon dates were obtained from macrofossils from unit L2 (Table 3 and Figure 6). The oldest date immediately above the distinct boundary between L1 and L2 on core JM07-012 suggests that the transition from glacier-proximal to glacier-distal conditions occurred prior to 9220 ± 160 cal. yr BP. Core JM07-014 does not penetrate through VK5, thus indicating that the transition from unit VK4 to VK5 occurred prior to 2930 ± 130 cal. yr BP (Figures 4 and 6 and Table 3).

The age–depth models for both cores are based on a linear fit between each of the radiocarbon dates and their lower and higher 2σ limits (Figure 7 and Table 3). Three small age reversals occurred below 125 cm in core JM07-014. However, all ages were used in the age model, because the offsets of the ages are always within a 1σ range of the next younger and older date. Thus, the linear fit for the lower six radiocarbon dates in core JM07-014 is a linear regression. This regression line in core JM07-014 extends from the base of the core to 110 cm where the most prominent changes in the sediment properties occur (Figure 6), most likely associated with significant changes in accumulation rates. The linear fit was chosen for its simplicity and applicability for age–depth models with a low amount of data (Telford et al., 2004). The connection of the radiocarbon dates with the

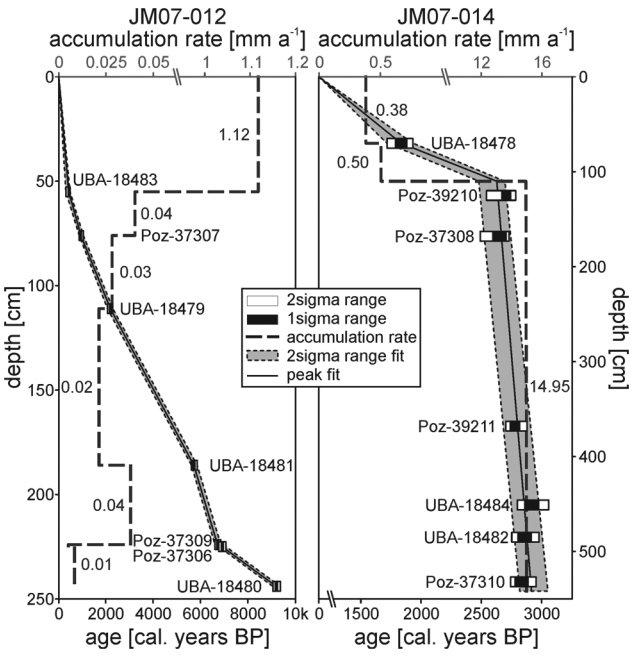

Figure 7. Age–depth models of the cores JM07-012 and JM07-014. Each radiocarbon date is represented with a 1σ (black) and a 2σ (white) bar, respectively. The laboratory code is written next to each sample. The grey area covers the area between the lower and higher 2σ limits within a linear fit.

debris-flow lobes is such that the stratigraphic level of both the upper boundary of the upper lobe and the base of the lower lobe are closely framed by radiocarbon dates. However, the sources of uncertainty of the ages of the lobes need to be considered, as there is (1) the uncertainty of radiocarbon dating; (2) the error in the reference depth on the sub-bottom profiles, though the p-wave velocity is not complex (Figure 6); and (3) the age reversals in the sequence of the radiocarbon dates, though they are within 1σ ranges. From this crude error assessment, it is not possible to put error bars on the age of the lobes, nevertheless need these uncertainties be kept in mind.

The accumulation rates of core JM07-012 are generally low (approximately 0.03 mm/a) during the early and mid-Holocene, which may be due to bottom currents at the fjord mouth, leading to reduced deposition and/or erosion. Only during the last *c*. 400 years, the accumulation rates increased more than one order of magnitude (1.12 mm/a). Similar changes in accumulation rates are described from other Spitsbergen fjords (Baeten, 2007; Hald et al., 2004).

In the eastern part of the outer basin (site JM07-014), extremely high accumulation rates prevail between 2930 and 2610 cal. yr BP (14.95 mm/a). The accumulation rates drop to 0.5 mm/a afterwards and decrease further to 0.38 mm/a between 1825 cal. yr BP and present.

Discussion

The late Weichselian/early Holocene deglaciation

The deglaciation of van Keulenfjorden began shortly before 11.8 cal. ka BP (Bratlie, 1994). The transverse ridges south of Ulladalen (Figure 2) and the esker beads with the v-shaped ridges further east in the outer basin are evidence for a stepwise retreat of the ice front. Glacier proximal conditions with frequent lithological changes (lithological unit L1; seismostratigraphic unit VK2) prevailed in the fjord during the deglaciation.

The high IRD content in unit L1 (Figure 6) is suggested to reflect enhanced ice-rafting during deglaciation. Ice-rafting occurred most probably from icebergs that calved off the retreating ice front and to a smaller degree from sea ice (cf. Forwick and Vorren, 2009; Hald et al., 2004).

The transverse ridges and the esker beads have a similar spacing as annual recessional moraines in other Spitsbergen fjords (Baeten et al., 2010; Boulton, 1986; Boulton et al., 1996; Ottesen and Dowdeswell, 2006, 2009; Ottesen et al., 2008), which is why they are interpreted to represent annual halts and/or re-advances of the generally retreating ice front. An eastward increase of the spacings from 80 to 190 m indicates that the annual retreat rate more than doubled during the deglaciation of the outer basin. Such an acceleration at the end of the last glacial might have been caused by a rising equilibrium line altitude due to climatic warming (Mangerud and Landvik, 2007) and/or a stronger inflow of warm AW into the fjord (cf. Hald et al., 2004; Rasmussen et al., 2012; Skirbekk et al., 2010) or other mechanisms. The maximum retreat rate in the outer basin correlates well with the retreat rates in Billefjorden (170 m/a; Baeten et al., 2010) and Smeerenburgfjorden (140 m/a; for location see Figure 1; Velle, 2012).

Assuming that the retreat rates of 80 and 190 m/a are constant for their areas of occurrence, and applying this combined retreat rate, the entire outer basin of van Keulenfjorden (approximately 22 km long) would have been deglaciated within ~210 years, that is, around 11.6 cal. ka BP.

The culmination of the deglaciation cannot be estimated from the existing data set. However, multiple studies from West Spitsbergen fjords, including the neighbouring van Mijenfjorden, suggest that the retreat of the glacier fronts towards the fjord heads terminated around 11.3–11.2 cal. ka BP (e.g. Baeten et al., 2010; Forwick and Vorren, 2009; Hald et al., 2004; Mangerud et al., 1992; Svendsen et al., 1996). Therefore, it is reasonable to assume that also the retreat of the glaciers in van Keulenfjorden terminated around this time.

Holocene sedimentary environments and glacial dynamics

The westward thinning of the postglacial succession (Figure 5d) suggests that the majority of the sediments derived from turbid waters emanating from Nathorstbreen at the fjord head. Since Nathorstbreen is a polythermal glacier (Hagen et al., 1993) meltwater input occurs throughout the year. However, the runoff is highly seasonal, and glacier surges can culminate with a considerable meltwater and, therewith, sediment flux (Svendsen et al., 2002).

Contrary to other studies from Spitsbergen fjords revealing increases in the average sedimentation rates during the past few millennia (e.g. Baeten et al., 2010; Forwick and Vorren, 2009; Hald et al., 2004; Skirbekk et al., 2010; Svendsen and Mangerud, 1997), the sedimentation rates in the eastern part of the outer basin in van Keulenfjorden dropped by about an order of magnitude from approximately 3.7 mm/a (approximately 30 m during *c*. 9 ka between the deglaciation and 2.61 ka BP) to approximately 0.4 mm/a at *c*. 2.61 cal. ka BP (disregarding the extremely high accumulation rate of 14.95 mm/a during the surge-like advances). This dramatic change resulted most probably from the modification of the large-scale basin morphology in van Keulenfjorden due to the deposition of a terminal moraine at the end of a surge-like advance of Nathorstbreen around 2610 cal. yr BP. Prior to that advance, the entire fjord comprised a single basin, where sediments were distributed relatively evenly. However, after the advance, the moraine divided the fjord into an inner and outer basin and acted as a barrier trapping the majority of the sediment between the proximal side of the moraine and the glacier front, thus leading to significantly reduced sedimentation rates in the outer basin.

Ottesen et al. (2008) suggest that the large lobe in the eastern part of the study area was deposited in relation to surge advances of Nathorstbreen during the late Holocene and that the upper lobe was deposited at the termination of a surge during the late 19th century. There is no reason to doubt their interpretation that the deposition of the lobes was related to advances of the glacier front and sediment reworking during surge advances. However, the correlation of the seismic reflections continuing from the top of the upper lobe and the base of the lower lobe, respectively, with core JM07-014 indicate that both lobes were deposited during the period of high accumulation rates between *c*. 2790 and 2610 cal. yr BP (Figures 4b and 6). Since there are no indications of sediment reworking in core JM07-014 and on the seismic profiles at the coring site, the core chronology is considered reliable. Thus, our results reveal that the lobes were deposited approximately 2600 years earlier than previously suggested.

High-resolution seismic data crossing the terminal surge moraine are not available. However, Ottesen et al. (2008) present a narrow corridor of swath-bathymetry data revealing an approximately 2-km-wide moraine complex bisecting the fjord basin. Multiple studies of landform assemblages in West Spitsbergen fjords related to glacier surges during the LIA and later reveal terminal moraines (typically <1 km wide) and one or multiple debris lobes on the distal sides of these moraines (e.g. Hald et al., 2001; Kristensen et al., 2009; Ottesen and Dowdeswell, 2006; Ottesen et al., 2008; Plassen et al., 2004). It is therefore assumed that the front of Nathorstbreen did not reach the westernmost crest of the moraine complex at the end of its surge in the late 19th century, but that it terminated to the east of it. The reworked material transported by the advancing ice front was most probably plastered to the proximal slope of the moraine complex that formed during the surge advances between 2790 and 2610 cal. yr

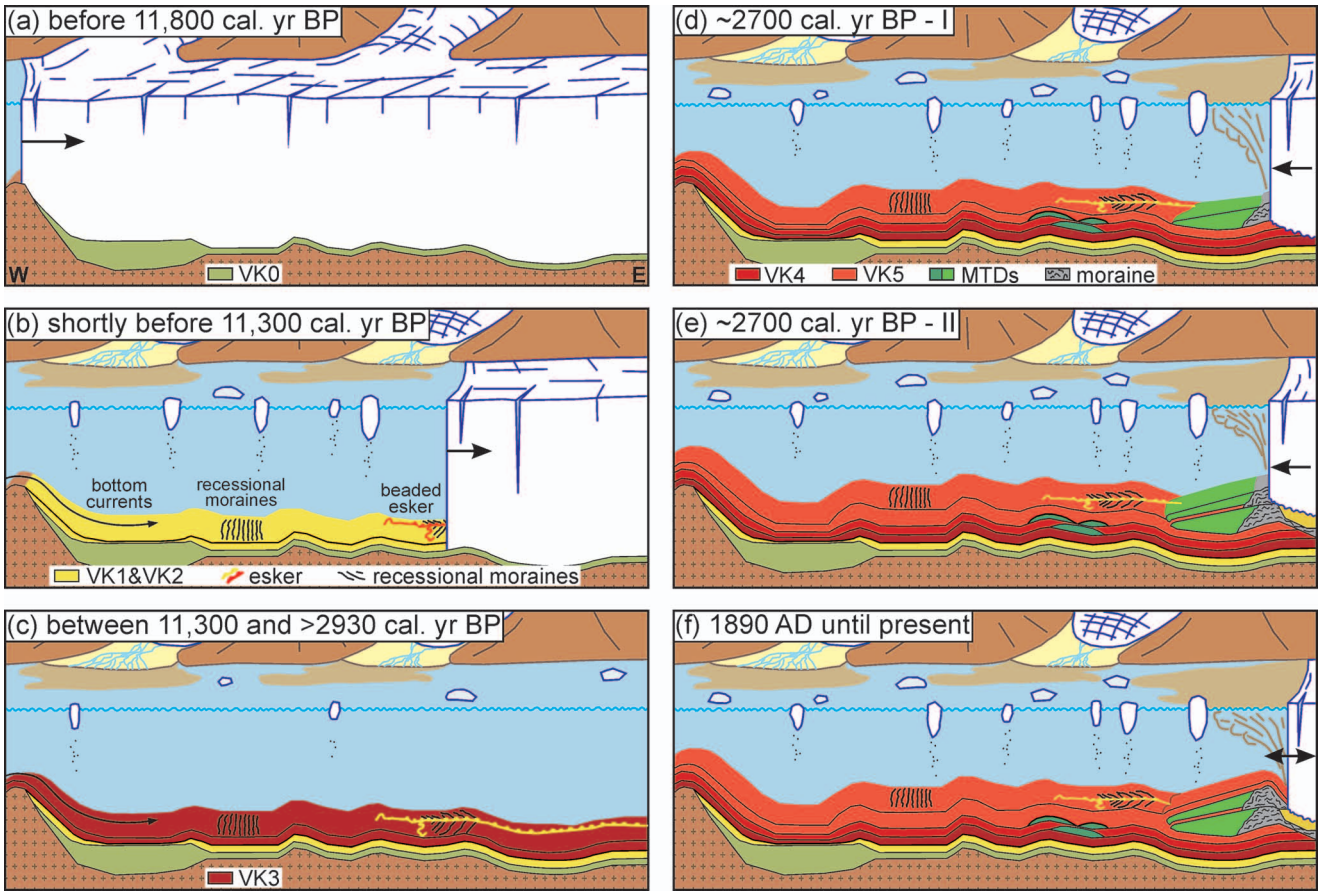

Figure 8. Sketch, summarizing the sedimentary processes, landforms and the glacial activity in the outer basin of van Keulenfjorden from the late Weichselian to the present. (a) before 11,800 cal. yr BP, (b) shortly before 11,300 cal. yr BP, (c) between 11,300 and >2930 cal. yr BP, (d) ~2700 cal. yr BP – I, (e) ~2700 cal. yr BP – II and (f) 1890 AD until present.

BP, indicating that this moraine complex had accumulated from repeated advances, for example, as in van Mijenfjorden (Ottesen et al., 2008).

Our results provide – to our knowledge – the oldest evidence of surge-like glacier advances on Svalbard. These advances occurred during a multimillennial period with the coldest environmental conditions on Svalbard during the Holocene that lasted from *c*. 4.7 to 2.0 cal. ka BP (Birks, 1991; Hald et al., 2004; Rasmussen et al., 2012; Skirbekk et al., 2010). However, most records of glacier surges on Svalbard date from the end of the LIA (e.g. Plassen et al. (2004), that is, from a period of general climatic warming). Based on these observations, we infer that glaciers on Svalbard can surge or advance surge-like in a variety of environmental conditions. The results show, furthermore, the importance of integrating swath-bathymetry and sub-bottom acoustic data, as well as lithological records to reliably date landforms that appear to be relatively young on swath-bathymetry data.

The time interval between the surges of Nathorstbreen around 2.7 ka BP was approximately 100–150 years, according to the measured thickness of acoustically stratified sediments and the inferred accumulation rate. Although a large error must be considered, this range fits well with the last and only historically known quiescent phase of Nathorstbreen of *c*. 120 years between the late 19th century and the most recent surge from 2003 to 2012 (Hagen et al., 1993; Sund et al., 2009, in preparation).

Conclusion

- During the last glacial, van Keulenfjorden was filled with a fast-flowing ice stream draining the Svalbard Barents Sea Ice Sheet.
- The deglaciation of the fjord commenced shortly before 11.8 cal. ka BP (Bratlie, 1994) and terminated around 11.3 cal. ka BP. The retreat of the ice front accelerated from 80 m/a in the western part of the outer basin to 190 m/a in its eastern parts (Figure 8a and b).
- Ice rafting was reduced between 11.3 cal. ka BP and before 2930 cal. yr BP (Figure 8c).
- Two sediment lobes were deposited in relation to surge-like glacier advances between *c*. 2790 and 2610 cal. yr BP. The lobes are – to our knowledge – the oldest surge-like advance deposits on Svalbard. The surge-like advance that led to the deposition of the upper debris lobe occurred approximately 2.6 ka earlier than previously suggested and indicates that surge-like glacier advances on Svalbard can occur under various climatic regimes (Figure 8d and e).
- The surge of Nathorstbreen during the late 19th century (Ottesen et al., 2008) terminated east of the existing moraine complex and did not have a significant influence on sedimentation rates in the outer basin of van Keulenfjorden (Figure 8f).
- The moraines from *c*. 2.7 ka had a large impact on the sediment distribution in the fjord, leading to a reduction in accumulation rates by one order of magnitude in the eastern part of the outer basin.

Acknowledgements

The captains and crews of RV *Jan Mayen* (now *Helmer Hanssen*) are thanked for their assistance during data collection. Steinar Iversen, Knut Sandaker, Roy Robertsen, Kyrre Lydersen, Jan P Holm and Trine Dahl provided technical support during and after the cruises. Maria Włodarska-Kowalczuk (Institute of

Oceanology, Polish Academy of Science, Sopot, Poland) carried out the taxonomical identification of the dating material. Al Werner and two anonymous reviewers are thanked for detailed and constructive comments. We extend our most sincere thanks to these people and institutions.

Funding

Det norske oljeselskap ASA provided funding to PK and MF The Research Council of Norway provided funding to JSL and TOV.

References

Baeten NJ (2007) *Late Weichselian and Holocene sedimentary processes and environments in Billefjorden, Svalbard*. Master Thesis, Department of Geology, Universitetet i Tromsø, Norway, 109 pp.

Baeten NJ, Forwick M, Vogt C et al. (2010) *Late Weichselian and Holocene sedimentary environments and glacial activity in Billefjorden, Svalbard.* Special Publication 344. London: The Geological Society of London, pp. 207–223.

Birks HH (1991) Holocene vegetational history and climatic change in west Spitsbergen – Plant macrofossils from Skardtjørna, an Arctic lake. *The Holocene* 1: 209–218.

Boulton GS (1986) Push-moraines and glacier-contact fans in marine and terrestrial environments. *Sedimentology* 33: 677–698.

Boulton GS, VanderMeer JJM, Hart J et al. (1996) Till and moraine emplacement in a deforming bed surge – An example from a marine environment. *Quaternary Science Reviews* 15: 961–987.

Bratlie B (1994) *Senkvatære sedimenter og glasialhistorie i Van Keulenfjorden, Svalbard*. Master Thesis, Institutt for Geologi, Universitetet i Oslo, Norway, 124 pp.

Carlson PR (1989) Seismic-reflection characteristics of glacial and glacimarine sediment in the Gulf of Alaska and adjacent fjords. *Marine Geology* 85: 391–416.

Dallmann WK, Hjelle A, Ohta Y et al. (1990) *Geological Map of Svalbard 1:100,000 Sheet B11G Van Keulenfjorden*. Oslo: Norsk Polarinstitutt.

Dallmann WK, Nagy J and Salvigsen O (1994) *Geological Map of Svalbard 1: 100,000, Sheet C11G Kvalvågen, Sheet C12G Markhambreen*. Oslo: Norsk Polarinstitutt.

D'Andrea WJ, Vaillencourt DA, Balascio NL et al. (2012) Mild Little Ice Age and unprecedented recent warmth in an 1800 year lake sediment record from Svalbard. *Geology* 40: 1007–1010.

Diemer JA (1988) Subaqueous outwash deposits in the Ingraham Ridge, Chazy, New York. *Canadian Journal of Earth Sciences* 25: 1384–1396.

Dowdeswell JA, Elverhøi A and Spielhagen R (1998) Glacimarine sedimentary processes and facies on the Polar North Atlantic margins. *Quaternary Science Reviews* 17: 243–272.

Elverhøi A, Lønne Ø and Seland R (1983) Glaciomarine sedimentation in a modern fjord environment, Spitsbergen. *Polar Research* 1: 127–149.

Elverhøi A, Svendsen JI, Solheim A et al. (1995) Late Quaternary sediment yield from the high Arctic Svalbard area. *The Journal of Geology* 103: 1–17.

Evans DJA and Twigg DR (2002) The active temperate glacial landsystem: A model based on Breiðamerkurjökull and Fjallsjökull, Iceland. *Quaternary Science Reviews* 21: 2143–2177.

Forwick M and Vorren TO (2007) Holocene mass-transport activity and climate in outer Isfjorden, Spitsbergen: Marine and subsurface evidence. *The Holocene* 17: 707–716.

Forwick M and Vorren TO (2009) Late Weichselian and Holocene sedimentary environments and ice rafting in Isfjorden, Spitsbergen. *Palaeogeography, Palaeoclimatology, Palaeoecology* 280: 258–274.

Forwick M and Vorren TO (2010) Stratigraphy and deglaciation of the Isfjorden area, Spitsbergen. *Norwegian Journal of Geology* 90: 163–179.

Forwick M and Vorren TO (2012) Submarine mass wasting in Isfjorden, Spitsbergen. In: Yamada Y, Kawamura K, Ikehara K et al. (eds) *Submarine Mass Movements and Their Consequences*. Springer, pp. 711–722.

Forwick M, Baeten NJ and Vorren TO (2009) Pockmarks in Spitsbergen fjords. *Norwegian Journal of Geology* 89: 65–77.

Forwick M, Vorren TO, Hald M et al. (2010) *Spatial and temporal influence of glaciers and rivers on the sedimentary environment in Sassenfjorden and Tempelfjorden, Spitsbergen*. Special Publication 344. London: The Geological Society of London, pp. 163–193.

Gilbert GR and Barrie JV (1985) Provenance and sedimentary processes of ice-scoured surficial sediments, Labrador Shelf. *Canadian Journal of Earth Sciences* 22: 1066–1079.

Hagen JO, Liestøl O, Roland E et al. (1993) *Glacier Atlas of Svalbard and Jan Mayen*. Meddelelser 129, Norwegian Polar Institute. Tromsø: Norsk Polarinstitutt.

Hald M, Dahlgren T, Olsen TE et al. (2001) Late Holocene palaeoceanography in Van Mijenfjorden, Svalbard. *Polar Research* 20: 23–35.

Hald M, Ebbesen H, Forwick M et al. (2004) Holocene paleoceanography and glacial history of the West Spitsbergen area, Euro-Arctic margin. *Quaternary Science Reviews* 23: 2075–2088.

Hansbo S (1957) *A New Approach to the Determination of the Shear Strength of Clay by the Fall Cone Test* (Royal Swedish Geotechnical Institute Proceedings 14). Royal Swedish Geotechnical Institute, pp. 1–49.

Hart JK and Watts RJ (1997) A comparison of the styles of deformation associated with two recent push moraines, South Van Keulenfjorden, Svalbard. *Earth Surface Processes and Landforms* 22: 1089–1107.

Henderson PJ (1988) Sedimentation in an esker system influenced by bedrock topography near Kingston, Ontario. *Canadian Journal of Earth Sciences* 25: 987–999.

Hooke RL and Elverhøi A (1996) Sediment flux from a fjord during glacial periods, Isfjorden, Spitsbergen. *Global and Planetary Change* 12: 237–249.

Høyland KV (2009) Ice thickness, growth and salinity in Van Mijenfjorden, Svalbard, Norway. *Polar Research* 28: 339–352.

Humlum O, Elberling B, Hormes A et al. (2005) Late-Holocene glacier growth in Svalbard, documented by subglacial relict vegetation and living soil microbes. *The Holocene* 15: 396–407.

Jessen SP, Rasmussen TL, Nielsen T et al. (2010) A new Late Weichselian and Holocene marine chronology for the western Svalbard slope 30,000–0 cal years BP. *Quaternary Science Reviews* 29: 1301–1312.

Jiskoot H, Murray T and Boyle P (2000) Controls on the distribution of surge-type glaciers in Svalbard. *Journal of Glaciology* 46: 412–422.

Kristensen L, Benn DI, Hormes A et al. (2009) Mud aprons in front of Svalbard surge moraines: Evidence of subglacial deforming layers or proglacial glaciotectonics? *Geomorphology* 111: 206–221.

Landvik JY, Bondevik S, Elverhøi A et al. (1998) The last glacial maximum of Svalbard and the Barents Sea area: Ice sheet extent and configuration. *Quaternary Science Reviews* 17: 43–75.

Landvik JY, Mangerud J and Salvigsen O (1987) The Late Weichselian and Holocene shoreline displacement on the west-central coast of Svalbard. *Polar Research* 5: 29–44.

Liestøl O (1977) *Årbok 1977-Notiser: Årsmorener foran Nathorstbreen?* Longyearbyen: Norsk Polarinstitutt.

Mangerud J, Bolstad M, Elgersma A et al. (1992) The last glacial maximum on Spitsbergen, Svalbard. *Quaternary Research* 38: 1–31.

Mangerud J, Bondevik S, Gulliksen S et al. (2006) Marine C-14 reservoir ages for 19th century whales and molluscs from the North Atlantic. *Quaternary Science Reviews* 25: 3228–3245.

Mangerud J, Dokken T, Hebbeln D et al. (1998) Fluctuations of the Svalbard-Barents Sea ice sheet during the last 150 000 years. *Quaternary Science Reviews* 17: 11–42.

Mangerud JAN and Landvik JY (2007) Younger Dryas cirque glaciers in western Spitsbergen: Smaller than during the Little Ice Age. *Boreas* 36: 278–285.

Ottesen D and Dowdeswell JA (2006) Assemblages of submarine landforms produced by tidewater glaciers in Svalbard. *Journal of Geophysical Research* 111: F01016.

Ottesen D and Dowdeswell JA (2009) An inter–ice-stream glaciated margin: Submarine landforms and a geomorphic model based on marine-geophysical data from Svalbard. *Geological Society of America Bulletin* 121: 1647–1665.

Ottesen D, Dowdeswell JA and Rise L (2005) Submarine landforms and the reconstruction of fast-flowing ice streams within a large Quaternary ice sheet: The 2500-km-long Norwegian-Svalbard margin (57°–80°N). *Geological Society of America Bulletin* 117: 1033–1050.

Ottesen D, Dowdeswell JA, Benn DI et al. (2008) Submarine landforms characteristic of glacier surges in two Spitsbergen fjords. *Quaternary Science Reviews* 27: 1583–1599.

Plassen L, Vorren TO and Forwick M (2004) Integrated acoustic and coring investigation of glacigenic deposits in Spitsbergen fjords. *Polar Research* 23: 89–110.

Rasmussen TL, Forwick M and Mackensen A (2012) Reconstruction of inflow of Atlantic Water to Isfjorden, Svalbard during the Holocene: Correlation to climate and seasonality. *Marine Micropaleontology* 94–95: 80–90.

Reimer PJ, Baillie MGL, Bard E et al. (2009) IntCal09 and Marine09 radiocarbon age calibration curves, 0–50,000 years cal BP. *Radiocarbon* 51: 1111–1150.

Skirbekk K, Kristensen DK, Rasmussen TL et al. (2010) *Holocene Climate Variations at the Entrance to a Warm Arctic Fjord: Evidence from*

Kongsfjorden Trough, Svalbard (Special Publications 344). London: The Geological Society of London, pp. 289–304.

Stewart FS and Stoker MS (1990) Problems associated with seismic facies analysis of diamicton-dominated, shelf glacigenic sequences. *Geo-Marine Letters* 10: 151–156.

Stuiver M, Reimer PJ and Reimer RW (2010) Calib 6.0.*2*. Available at: http://www.calib.org

Sund M, Eiken T, Hagen JO et al. (2009) Svalbard surge dynamics derived from geometric changes. *Annals of Glaciology* 50: 50–60.

Sund M, Lauknes TR and Eiken T (in preparation) Surge dynamics in the Nathorstbreen glacier system, Svalbard.

Svendsen H, Beszczynska-Møller A, Hagen JO et al. (2002) The physical environment of Kongsfjorden–Krossfjorden, an Arctic fjord system in Svalbard. *Polar Research* 21: 133–166.

Svendsen JI and Mangerud J (1997) Holocene glacial and climatic variations on Spitsbergen, Svalbard. *The Holocene* 7: 45–57.

Svendsen JI, Elverhøi A and Mangerud J (1996) The retreat of the Barents Sea Ice Sheet on the western Svalbard margin. *Boreas* 25: 244–256.

Syvitski JPM and Praeg DB (1989) Quaternary sedimentation in the St. Lawrence Estuary and adjoining areas, Eastern Canada – An overview based on high-resolution seismo-stratigraphy. *Geographie Physique Et Quaternaire* 43(3): 291–310.

Telford RJ, Heegaard E and Birks HJB (2004) All age-depth models are wrong: But how badly? *Quaternary Science Reviews* 23: 1–5.

Velle JH (2012) Holocene sedimentary environments in Smeerenburgfjorden, Spitsbergen. Master Thesis, Department of Geology, Universitetet i Tromsø, 128 pp.

Vorren TO, Lebesbye E, Andreassen K et al. (1989) Glacigenic sediments on a passive continental margin as exemplified by the Barents Sea. *Marine Geology* 85: 251–272.

Warren WP and Ashley GM (1994) Origins of the ice-contact stratified ridges (eskers) of Ireland. *Journal of Sedimentary Research – Section A: Sedimentary Petrology and Processes* 64: 433–449.

Werner A (1993) Holocene moraine chronology, Spitsbergen, Svalbard: Lichenometric evidence for multiple Neoglacial advances in the Arctic. *The Holocene* 3: 128–137.